Electronic Supplementary Material (ESI) for Physical Chemistry Chemical Physics.

Supporting Information

Cis/trans-3α-hydroxypyrroloindole (HOPI) characterization

The structure of *cis/trans*-3α-hydroxypyrroloindole (HOPI) is given in Figure S2. The two observed diastereoisomers have the configurations R,R,S or S,S,S. The alpha carbon remains in the same S chirality, since the HOPI was obtained from L-tryptophan. Figure S3 shows the 1D ^{1}H NMR spectra of both diastereoisomers. The signals were assigned with the help of 2D homo and heteronuclear experiments shown in Figure S4. The [^{13}C,^{1}H]-HMQC, enabled the connection of ^{13}C-^{1}H moieties, while the [^{13}C,^{1}H]-HMBC allowed to correlate ^{13}C ^{1}H connections that are further apart, i.e. have smaller heteronuclear scalar couplings. Finally, the [^{1}H,^{1}H]-TOCSY correlates the scalar-coupled protons.

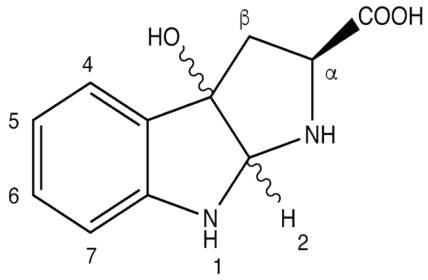

Figure S1: Structure of the Cis/trans-3α-hydroxypyrroloindole

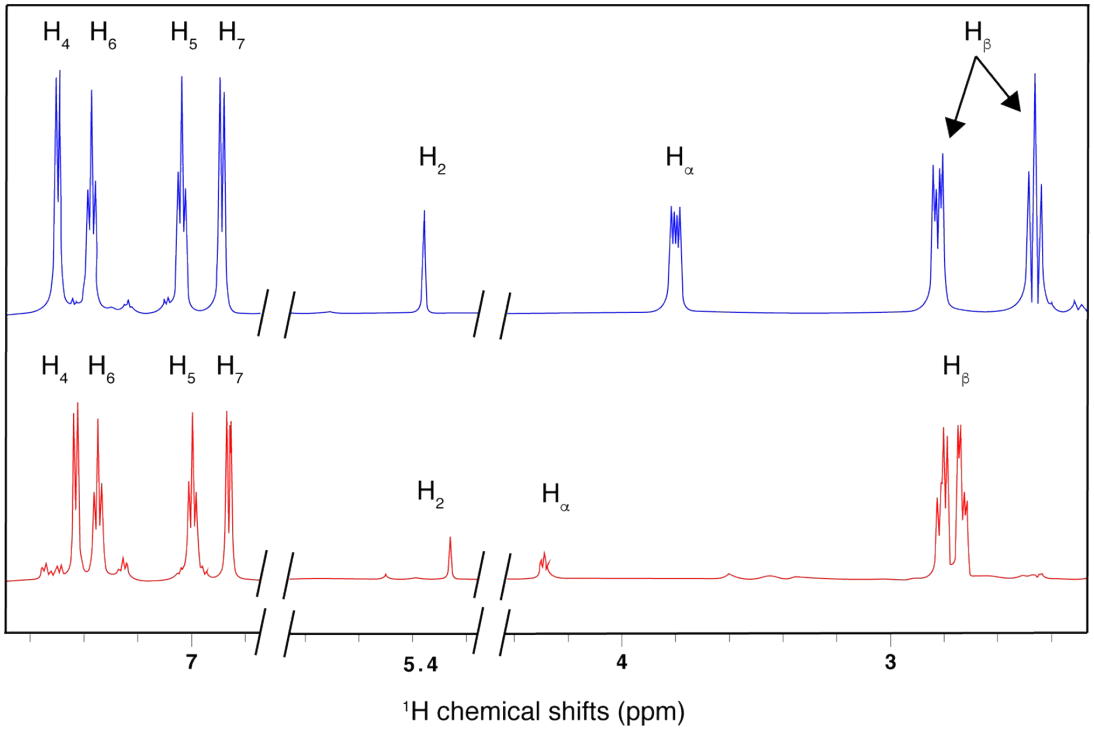

Figure S2: 1D ^{1}H NMR spectra of both diastereoisomers of HOPI with assignments. Upper spectrum is cis-HOPI, and lower is trans-HOPI. Both molecules were at 1 mM in H_2O, 100 mM KPO_4 buffer, pH = 7.1. Spectra were recorded with 128 scans, 16k points acquisition and 3 s recovery delay. The peaks H_2 and H_α are of low intensities due to the WATERGATE (w5) scheme used for water suppression which attenuate the signals close to the carrier.[1]

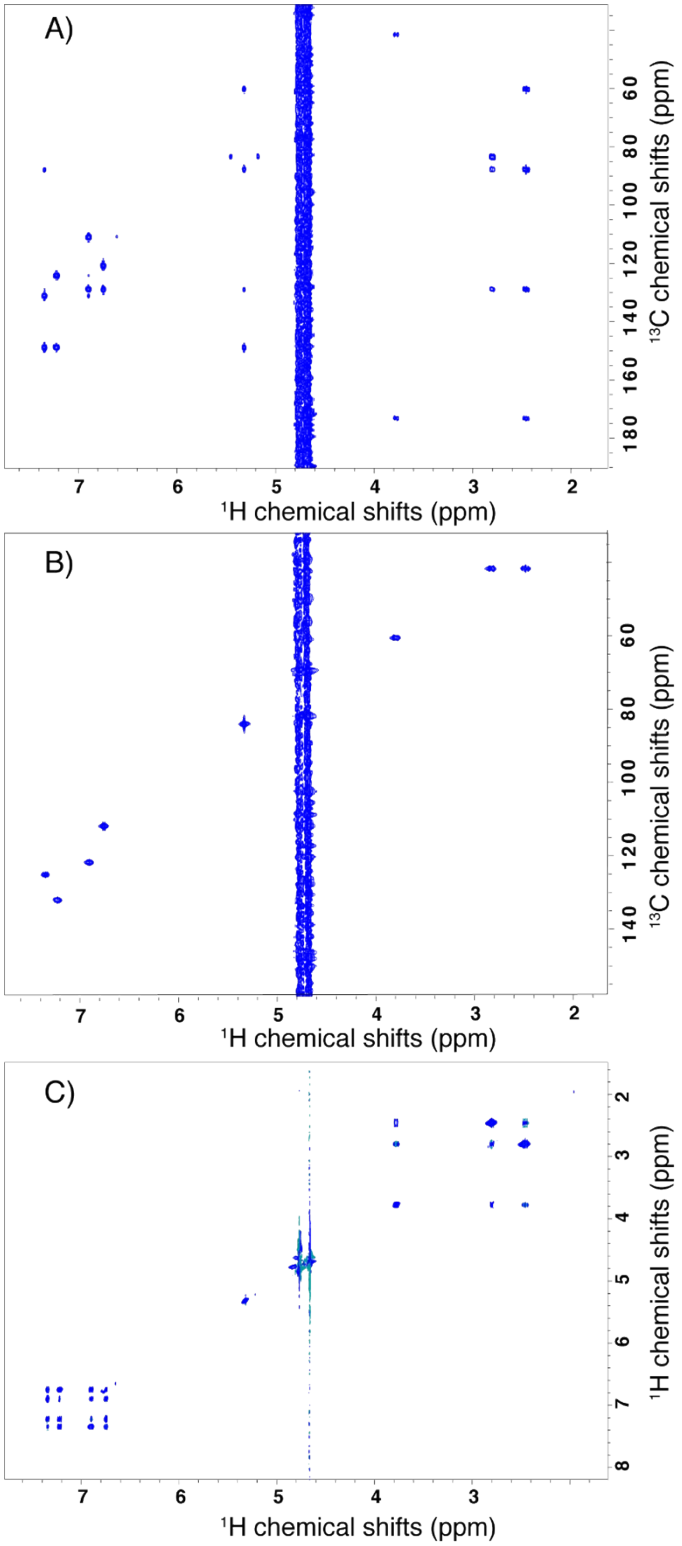

Figure S3: The HPLC purified fractions where analyzed with a set of state-of-the-art NMR experiments that enables one to establish the C-C and C-H connections and proximity and for the identification of the protons that belong to a scalar-coupled spin system A) Heteronuclear Multiple Bond Correlation B) Heteronuclear Multiple Quantum Correlation C) ^{1}H,^{1}H-TOtal Correlated SpectroscopY.

3α-hydroxypyrroloindole synthesis

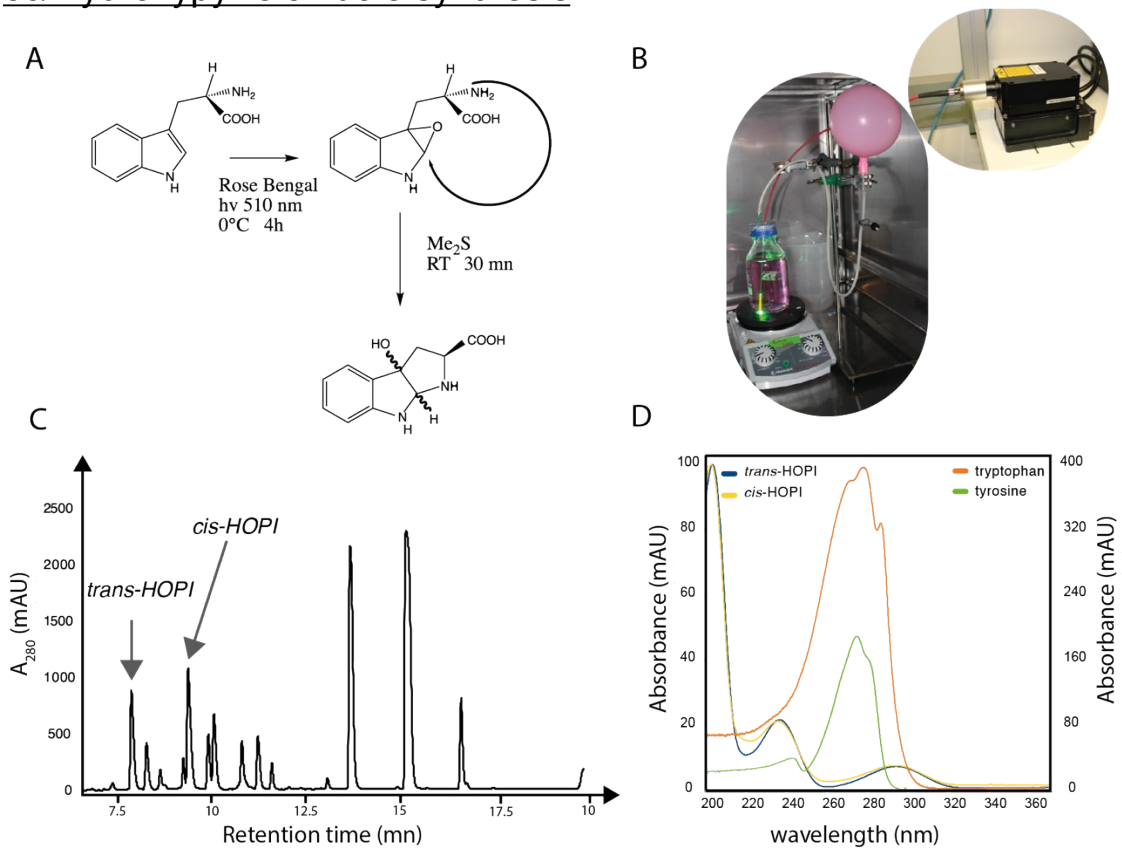

Figure S4: A) Reaction mechanism for the formation of the cis/trans-HOPI. B) Set up for the photo-oxidation of tryptophan. C) HPLC purification profile of HOPI from the tryptophan photo-oxidation reaction. D) UV absorption spectra for both diastereoisomers of HOPI compared to tryptophan and tyrosine. The maximal intensities were normalized to 100 mAu for visibility reasons. However, the tryptophan and tyrosine concentrations were 25 µM and the cis/trans-HOPI concentrations were of 50 µM. The left y-axis is referring to the cis- and trans-HOPI, and the right axis to the tryptophan and tyrosine.

The HOPI synthesis has been already described in the literature. In our case we used a LASER (532nm, 0.5W) as the irradiation source to generate $^{s}O2$ from rose Bengal (RB) and the RB was removed from the reaction mixture via C18 solid phase extraction (SPE) in place of a liquid-liquid extraction. The sample was not acidified for SPE so that the RB remained visible and it could be monitored visually on the SPE column. The final purification was done on a semi-preparative C18 column.

Tryptophan and tyrosine photo-CIDNP with AT12

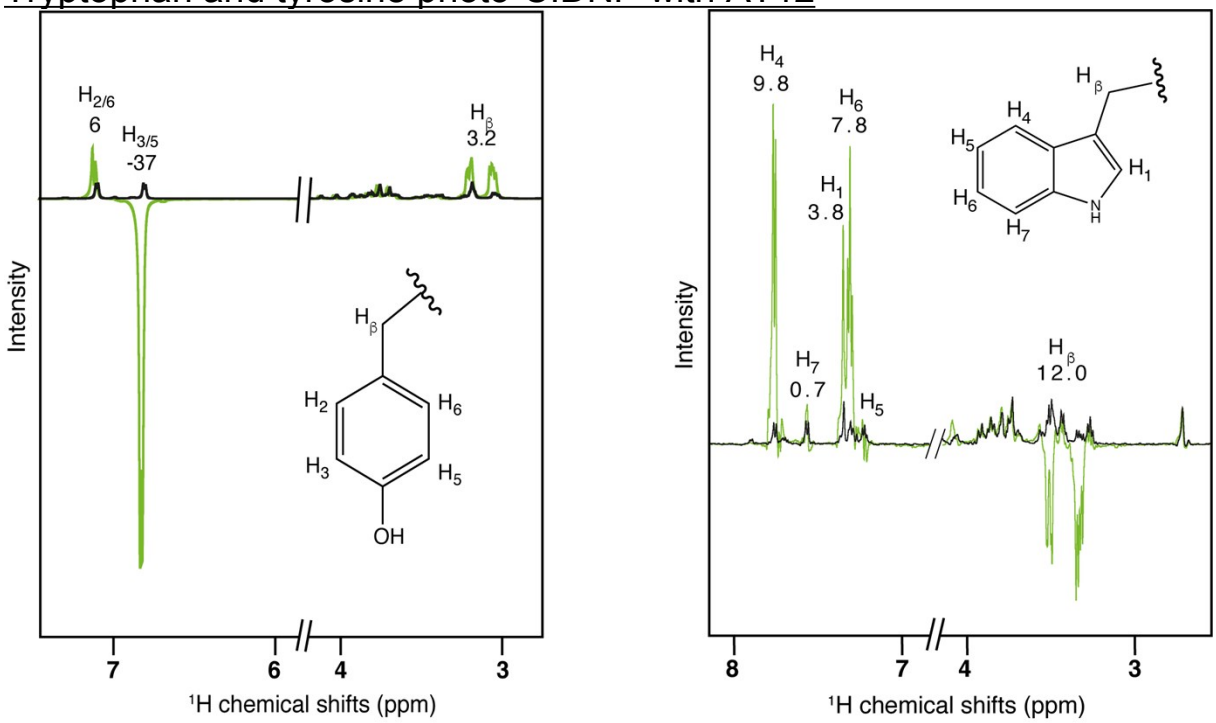

Figure S5 : Photo-CIDNP ¹H-NMR spectra of 100 µM tyrosine (left) and 100 µM tryptophan (right) in the presence of 20 µM of AT12. Dark spectra are in black color and irradiated spectra are in green color, respectively Irradiation was performed with a wavelength of 532 nm, during 4 s at power 1 W.

Reaction kinetics

The efficiency of photo-CIDNP is strongly dependent on the radical pair concentration originating from the electron transfer from the molecule to the triplet state dye. The formation of triplet state dye is the mandatory step prior to radical pair formation. In a first approximation, under laser irradiation, the triplet state dye (D) is formed in a steady state described by the following (1):

$$[D] = K[D_0] = \frac{k_{ex}k_{ISC}}{k_T(k_{fluo} + k_{ISC})}[D_0]$$

With $[D_0]$ the total dye concentration, the rate constants, k_{ex} for the formation of an excited singlet state, k_{ISC} for the intersystem crossing between the excited singlet state to the triplet state, k_{fluo} for the fluorescence, and k_T for the triplet-singlet relaxation.

Since it is a cyclic process, the photo-CIDNP can be simplified to a reversible reaction:

$$M + D \leftrightarrows RP$$

Where *M* is the molecule to be hyperpolarized, and *RP* is the radical pair. As stated above, due to the long irradiation time (seconds) practiced in the present study, the system is assumed to be in a steady-state, i.e. (2):

$$\frac{d[RP]}{dt} = 0$$

Hence, the solution to the equation of the bimolecular reaction (3):

$$\frac{d[RP]}{dt} = k_1[M][D] - k_{-1}[RP]$$

Is (4):

$$[RP] = \frac{k_1}{k_{-1}}[M][D]$$

Equation 4 describes the steady-state concentration in a reversible bimolecular reaction. The amount of *RP* is dependent on the concentration of both the *D* and *M*.

Moreover, the photo-CIDNP enhancement of tryptophan in the presence of HOPI (both *trans* or *cis)* has been studied (Figure S6). For increasing concentrations of HOPI, the enhancement of tryptophan decreases, evidence of a competition in the formation of the radical pairs. Furthermore, the quenching of the tryptophan photo-CIDNP is more pronounced with the more photo-CIDNP active *trans*-HOPI diastereoisomer. The competing reactivities of the photo-CIDNP active species underscore the importance of kinetics for the spin sorting process (see main text).

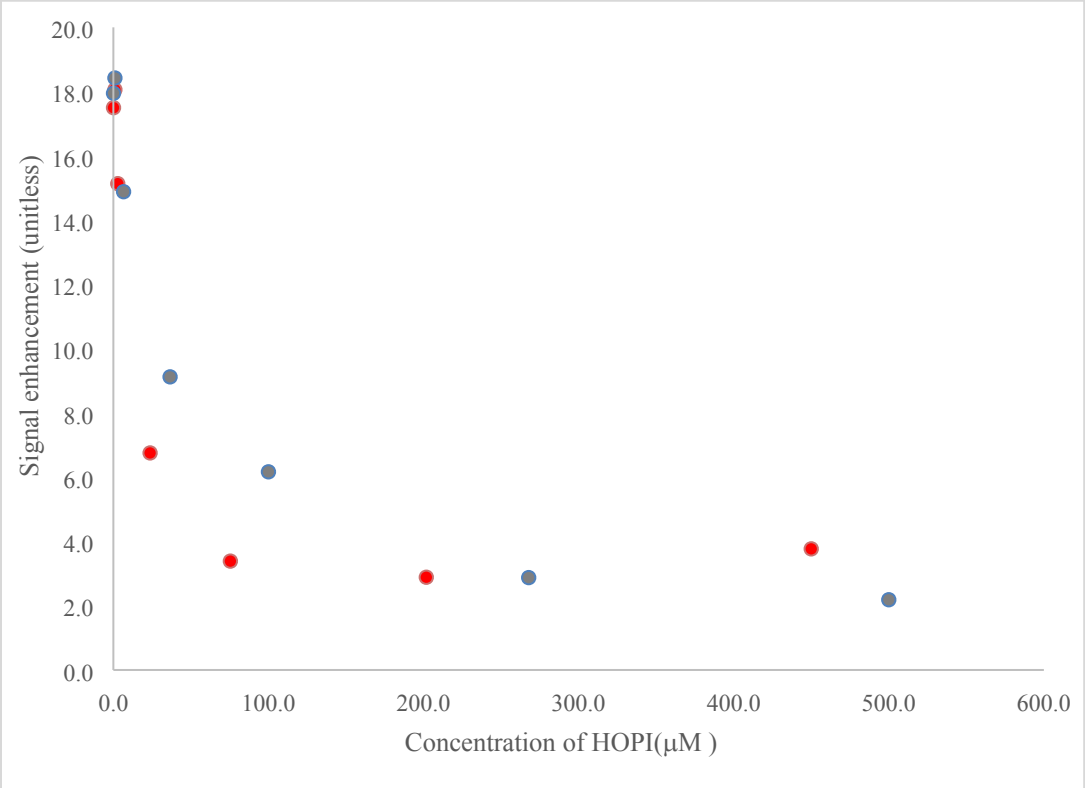

Figure S6: Quenching of the tryptophan (100μM) photo-CIDNP at 298 K with increasing concentration μM) of trans-HOPI (red) and cis-HOPI (grey).[2]

Time resolved photo-CIDNP experiments to determine CIDNP-relevant parameters

In a CW-photo-CIDNP experiment the predominance of F-Pair over geminate polarization slightly deviates the total polarization. This is the reason why, the exact physical parameters, HFC and g-factor difference, can only be calculated with time resolved (tr)-photo-CIDNP.[3] In contrast to CW-CIDNP studies tr-CIDNP allows to determine the reaction mechanism and the hyperfine coupling constants in transient radicals. 3,3′,4,4′-tetracarboxy benzophenone (TCBP) has been used in previous studies and is known to produce high photo-CIDNP enhancements, and HFCCs of which were well established. The NMR experiment was performed as following: a pre-saturation (WALTZ16) sequence prior to light irradiation by an 308 nm excimer laser and the CIDNP spectra is detected without any delay after the single short laser pulse (with duration of a few nanoseconds) using a short radio frequency pulse (typical duration of 1 μs). As shown previously,[4] the relative signal intensities in the geminate spectrum are proportional to the hyperfine coupling constants (HFCs) in the radicals constituting the geminate radical pair.

TCBP has been used as the photosensitizer for the following reasons:

1) its radicals have well determined hyperfine coupling constants known from EPR and our previous work;
2) because its radicals show clear CIDNP patterns, that are distinctly different for electron transfer (ET) and proton coupled electron transfer (PCET) reactions.

The Table S1 summarizes the radical species associated to ET or PCET as well as the corresponding apparent HFC enabling to evaluate the electron transfer mechanism.[5] Unfortunately, in the geminate CIDNP spectra of both compounds (Figure S7), *cis* and *trans* HOPI, an admixture of L-tryptophan was clearly visible. For elimination of the unwanted contribution from the reaction of TCBP with L-tryptophan to CIDNP reference geminate spectra from the reaction of TCBP with L-tryptophan and N-acetyl tryptophan have been used (Figure S7). Integration of the individual line intensities in the reference spectra allowed us to determine the relative contribution to CIDNP from L-Trp as 1:20 and to subtract it from the geminate CIDNP spectra of both HOPIs. The corrected spectra are shown in Figure S8.

The total signal intensities in geminate CIDNP spectra depend on the quenching rate constants and the CIDNP enhancement coefficients; the latter are determined by the lifetime of the geminate spin correlated radical pair and its magnetic resonance parameters. L-tryptophan with its positively charged amino group provides more efficient ^{3}TCBP quenching and a higher photo-CIDNP enhancement coefficient, resulting in higher photo-CIDNP signal intensities.[6] The amino group of N-Acetyl-tryptophan is uncharged. *cis*-HOPI and *trans*-HOPI have a pKa of 7.7 and are therefore in a mix, 62% protonated (positively charged) and 38% unprotonated (neutral). The CIDNP signal intensities of H2,2′ of TCBP in case of N-Acetyl- tryptophan, *cis*-HOPI and *trans*-HOPI correlate as 2.7:1:1.1 as seen in Figures S7 and S8.

For TCBP, the experimentally determined values -0.252 mT (H6,6′), -0.209 mT (H2,2′), 0.067 mT (H5,5′) were taken. These values correspond to the combination of radical **T-I, T-III**, and **T-IV** (Figure S10), which is indicative of PCET (proton coupled electron transfer)

as the reaction mechanism (by contrast to the case of L-tryptophan, when ET results in correlation with the **T-I** radical alone).[7] The correlation plots are given in the main part as Figure 5.

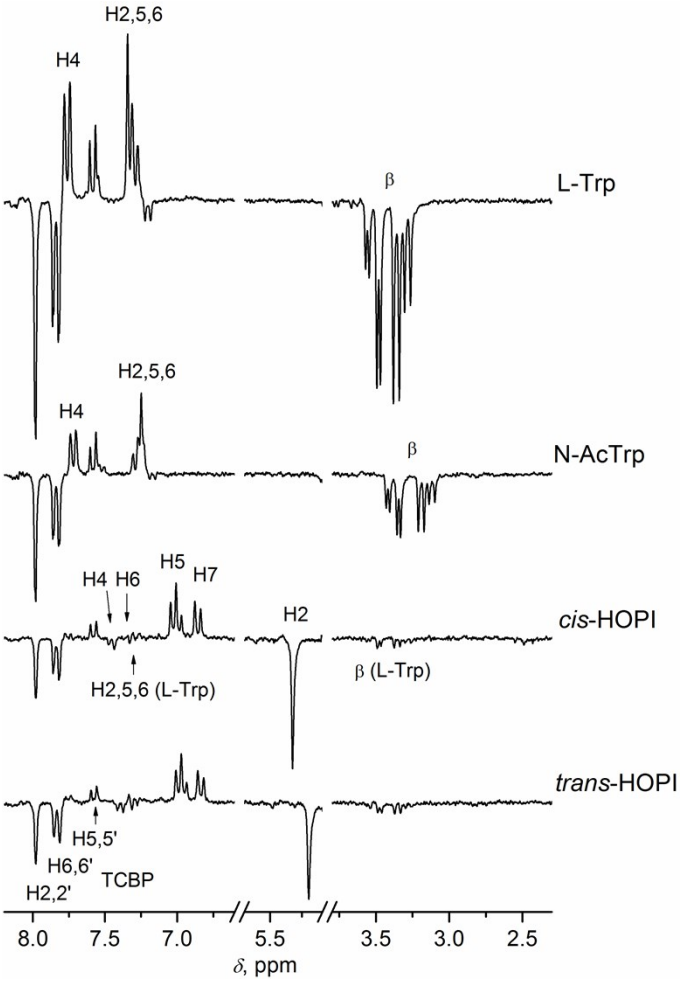

Figure S7: 200 MHz ^{1}H CIDNP spectra, obtained in the photoreaction between 4 mM TCBP and 4 mM L-Trp, 2 mM N-AcTrp, ~4 mM cis-HOPi and ~4 mM trans-HOPI at neutral pH. Spectra were recorded with no delay after the laser pulse using a detecting RF pulse of 1 μs, thus they contain only signals of the geminate reaction products.

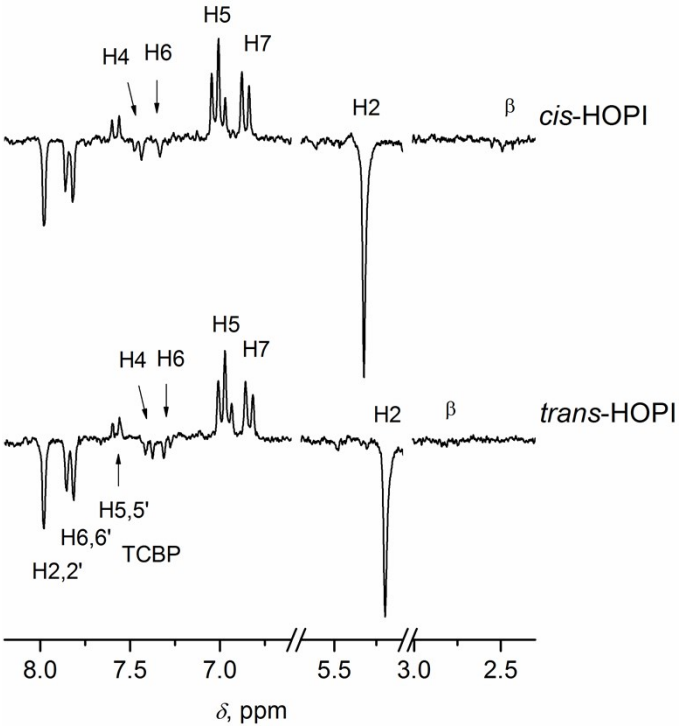

Figure S8: Spectra from Fig. S7, but with a subtracted geminate spectrum of CIDNP detected in reaction of TCBP with L-Trp (shown in Figure S7) divided by a factor of ~ 20 adjusted to achieve zero contribution from CIDNP in reaction of TCBP with L-Trp. The estimated concentration of L-Trp in the samples with HOPI is therefore ~ 0.2 mM.

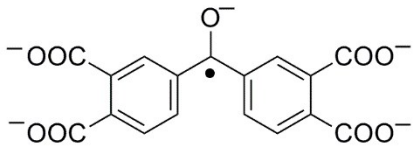

T-I

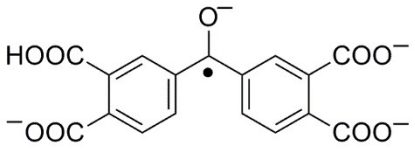

T-III

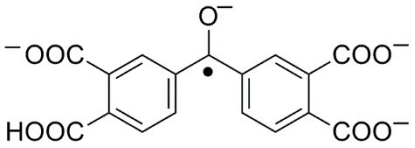

T-IV

k

Figure S9: Different radical of TCBP that can be generated depending on the radical formation mechanism ET of PCET.

Table S1: HFCCs (mT) for the protons of TCBP radicals.

Mechanism	Radical	H2,2′	H6,6′	H5,5′
ET	T-I	-0.253	-0.265	0.0897
PCET	T-I:T-III:T-IV= 0.56:0.18:0.25	-0.209	-0.252	0.068

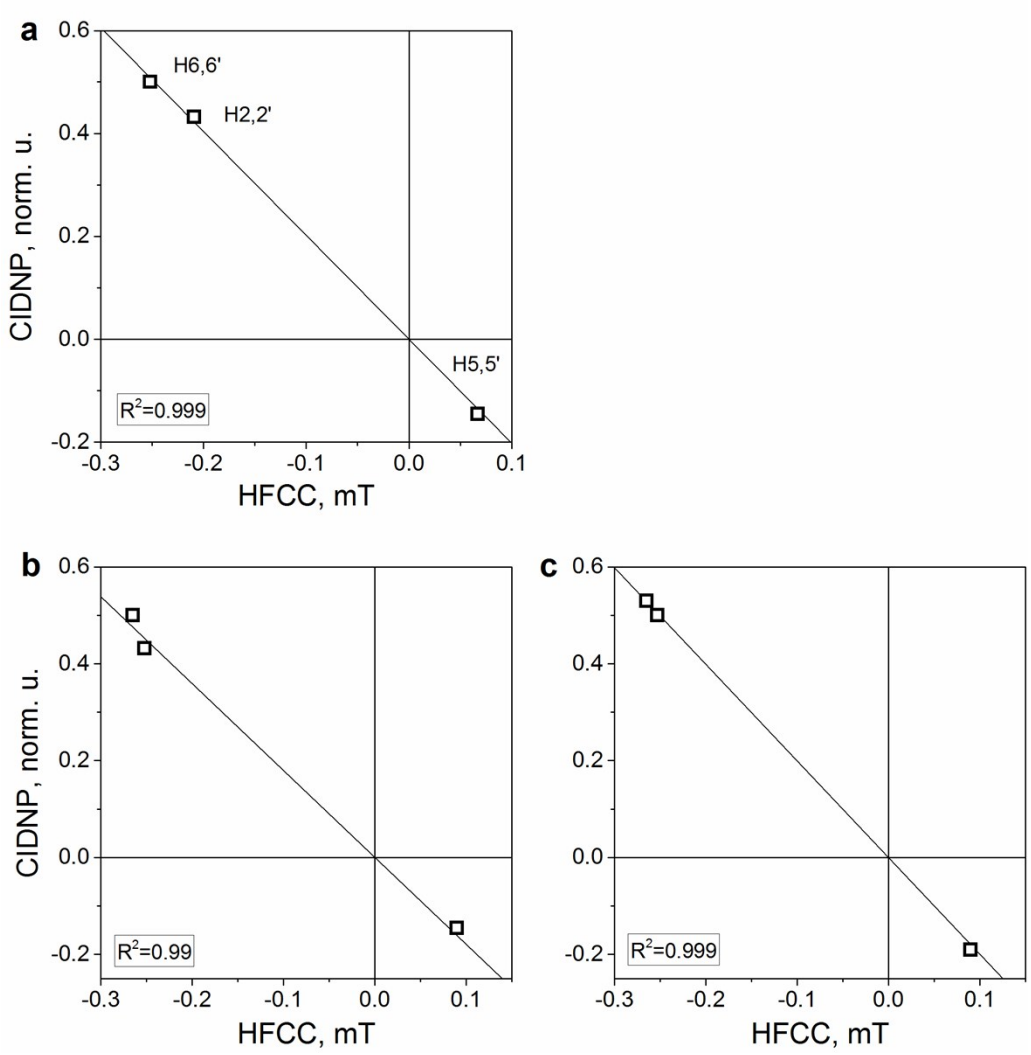

*Figure S10: A) Correlation between ^{1}H CIDNP intensities of TCBP detected in the photoreaction of TCBP and trans-HOPI, and the HFCCs of the protons of TCBP radicals **T-I:T-III:T-IV**=0.56:0.18:0.25. B) correlation between ^{1}H CIDNP intensities of TCBP detected in the photoreaction of TCBP and trans-HOPI, and the HFCCs of the protons of TCBP anion **T-I**. C) correlation between ^{1}H CIDNP intensities of TCBP detected in the photoreaction of TCBP and N-AcTrp, and the HFCCs of the protons of TCBP anion **T-I**. Solid line: best fit by the function $P_{2j}=-C_2A_{2j}$.*

It is finally noted here that the impressive performances of HOPI in the CW-photo-CIDNP experiment using AT12 (Table 1) appears to be at odds to the tr-photo-CIDNP experiments in the presence of TCBP where the HOPI compounds are less enhanced as compared to tryptophan or N-acetyl-tryptophan. These apparent disappointing performances seems to be related to the different dyes and conditions used. About the latter, the tr-photo-CIDNP experiments are performed at mM concentration for which trans-HOPI shows less enhancement also with AT12 (Figure 4C) and solely the geminate polarization is present as it is necessary for the fine analysis of the radical parameters. Moreover, the time resolved experiments were performed at pH = 7.5 resulting into 62% HOPI/H^+ while the CW experiments were performed at pH = 7.1 resulting into 80% HOPI/H^+. The photo-CIDNP effect has been observed to be 2.5 times higher when performed in more acidic conditions.

Simulation of hyperfine couplings (HFCs) and g-factors

To calculate the hyperfine couplings simulations were run with the Gaussian® software with the Density Functional Theory (DFT) method. The geometries were first optimized with a quick molecular dynamics refinement using the UFF, and then with an unrestricted B3LYP functional and a 6-31+G(d,p) basis set in implicit water solvent (Polarizable Continuum Model, PCM). The HFCs were calculated with the EPR-III basis set.

Table S2: Hyperfine coupling constants (mT) for the radicals of trans-HOPI, cis-HOPI and cationic tryptophan (TRP)

Molecule	H2	H4	H5	H6	H7	Hb	Ha
trans-HOPI	1.047	0.229	-0.850	0.156	-0.498	0.141; -0.022	0.067
cis-HOPI	1.273	0.231	-0.853	0.138	-0.480	-0.021;0.035	0.014
TRP^+	-0.177	-0.168	0.028	-0.105	-0.061	0.364;0.016	-0.083

The g-factor calculations were run with the Gaussian® software with the DFT method. The geometries were optimized up to the 6-311+G(2d,2p) level. Implicit water solvent was used as well (PCM). Then computed with the nmr=giao keyword. The approach presented is following published work on the computation of g-factors for small molecules[8]. The obtained values are displayed in the Table S3. However, it is important to keep in mind that g-factor calculations are typically rather inaccurate. We could obtain a reasonably close value to the literature value for tryptophan (2.0027)[3] with our method, but these values should be looked at with a qualitative rather than strictly quantitative eye. Nevertheless, the computed values of g-factor are consistent with the sign alternation observed when the dye is changed from fluorescein to AT12. However, since TCPB with a gactor of 2.0035 behaves like AT12, HOPI's g factors are rather in the vicinity of a little bit lower than 2.0035 (but larger than 2.0034). Figure S11 is the g-factor ranking chart, adapted from Sobol et al.[9], updates to contain the HOPI products.

Table S3: G-factors (unitless) were calculated with unrestricted B3LYP, 6-311+G(2d,2p) or aug-cc-pVTZ basis set and implicit water solvation (PCM) for the cis/trans-HOPI, and cationic TRP radicals.

Molecule	6-	Aug-cc-pVTZ

	311+G(2d,2p)	
trans-HOPI	2.0035527	2.0035566
cis-HOPI	2.0035831	2.0035872
TRP^+	2.0028128	2.0028144

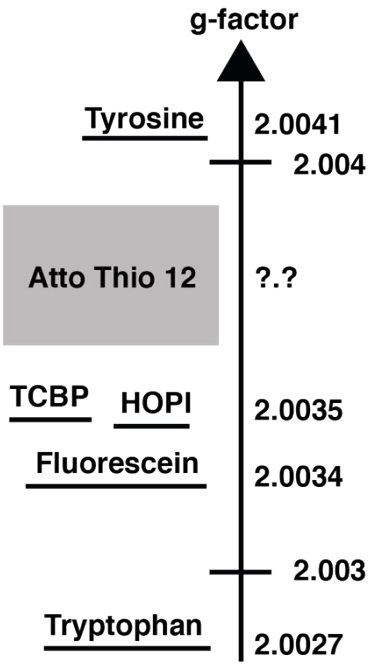

Figure S11: Ranking of the molecules according to their respective g-factor, adapted from Sobol et al.[9]

Longitudinal (T1) relaxation of the *cis*/*trans*-HOPI compounds

The T1 relaxation of the different HOPI diastereoisomers has been measured with NMR. The data were recorded using the Topspin pulse sequence (t1ir) modified to introduce a w5 water suppression scheme and the relaxation time were fitted with the fitting tool from Topspin 3.2.

The two diastereoisomers exhibit very close relaxation properties, which is expected. Interestingly the H2 proton of the cis-HOPI has a slightly slower T1 relaxation as compared to the trans-HOPI which is in opposition to the initial thought that an internal H-bond formation would rigidify the structure. The internal H-bond formation for the *cis*-HOPI is very unlikely. Otherwise, the T1 relaxation time for the H2 would be significantly faster than for the *trans*-HOPI (Figure S12).

Bleaching of the CIDNP effect with *cis*/*trans*-HOPI compounds

A bleaching of the photo-CIDNP signal-to-noise enhancement (SNE) was observed by repeating the irradiation with a 1 min interval (Figure S13). There is a tremendous difference in the bleaching dynamics of the *cis*-HOPI which is fairly slow and the *trans*-HOPI. The bleaching can be also observed on the dye side, after the experiment the sample is transparent instead of purple as prior to irradiation. Furthermore, the 1D spectra before and after the series of irradiation show no difference in the amount of *cis*/*trans*-HOPI, suggesting that the bleaching is due to the dye degradation. This finding implies

two conclusions: first, the *cis*-HOPI is less reacting than the *trans*-HOPI which correlates with its relatively lower photo-CIDNP activity; second, the dye bleaching is the limiting factor of our photo-CIDNP system and is resulting from the interaction with the to-be-polarized molecule.

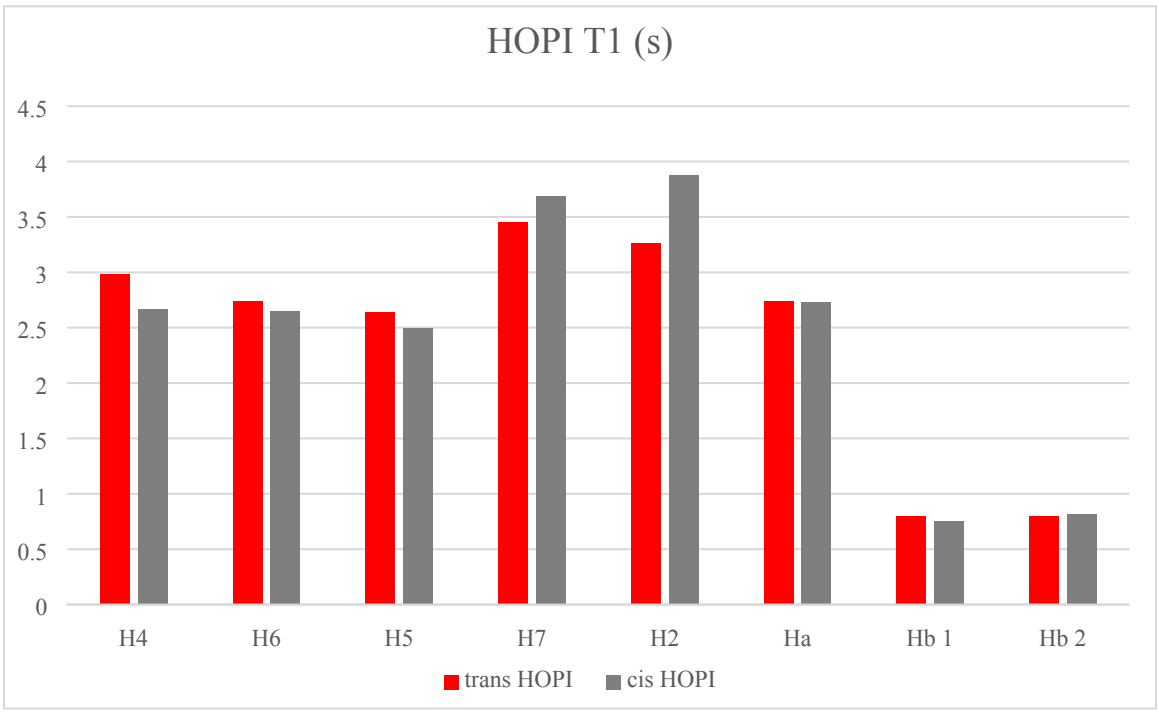

Figure S12: ^{1}H T1 (s) relaxation value of the different protons of the trans/cis-HOPI. The relaxation delay used were: 0.05, 0.10, 0.30, 0.50, 1.00, 1.50, 2.00, 3.00, 5.00, 8,00 seconds.

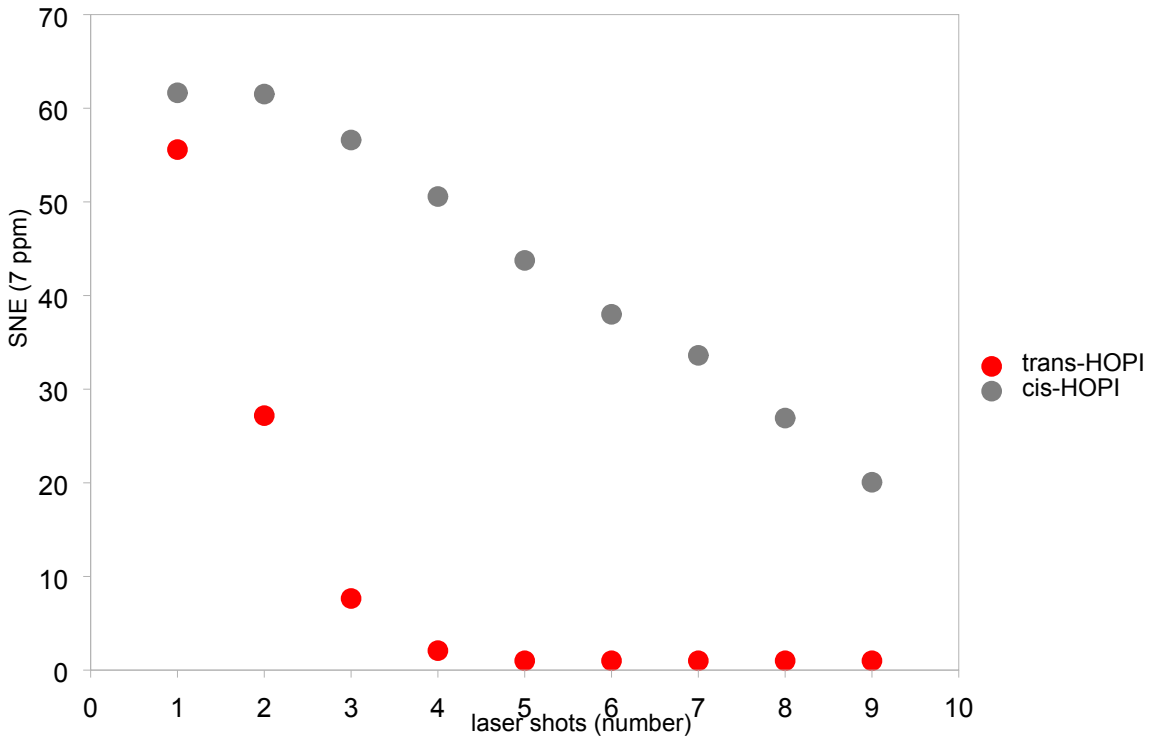

Figure S13: photo-CIDNP bleaching of cis/trans-HOPI (1 mM) compounds in the presence of AT12 monitored by the observation of H7. The laser pulses were repeated every 1min with an intensity of 1 W and a duration of 4s.

Photo-CIDNP experiments at 200 MHz

The signal to noise at 200 MHz for 100 μM *trans*-HOPI sample was so low that an accumulation of scans was necessary to estimate the irradiated 1 scan experiment signal enhancement. In this case the calculation was done as follows:

$$SE = \sqrt{NS} \times EF \qquad (5)$$

With *SE* as the signal enhancement, *NS* the number of scans, and *EF* the enhancement factor which is the apparent ratio of the signal intensities. We hence obtained for the proton H5 a signal enhancement of 381 for AT12 and 159 for the fluorescein photo-CIDNP experiments. It is important to note that the experimental time for the dark spectrum was 16 hours (11520 scans at 5 seconds per scan).

Proton detected carbon Photo-CIDNP at 600 MHz

The analysis was analogous to the 200 MHz experiments, but here because of the low natural abundance of ^{13}C and its lower gyromagnetic ratio, the signal from a 100 μM *trans*-HOPI sample was not detectable within 1 scan (Figure 6). We hence recorded an accumulation of 2560 scans and calculated the enhancement with equation 5. We estimated for the carbon C5 of *trans*-HOPI a signal enhancement of above 1000, the carbon C2 is showing an even greater enhancement, which we estimate to be of the order

of 1500-2000. Two interesting facts to note: all of the enhanced signals are emissive, meaning the sign of the HFC is positive. However, we can observe that the C7 and the C2 signals are absorptive for the minor conformations.

In the Figure S14 the ^{1}H photo-CIDNP and the [^{13}C polarized, ^{1}H detected]-photo-CIDNP experiments are displayed for comparison. The first INEPT block transfers the hyperpolarized carbon spin magnetization to the proton, to be detected after getting rid of the anti-phase term. The gradient enhanced pulse program enables the selection of the in-phase term in 1 scan without phase cycling. This pulse sequence is greatly inspired by the work of Cavagnero et al.[10]

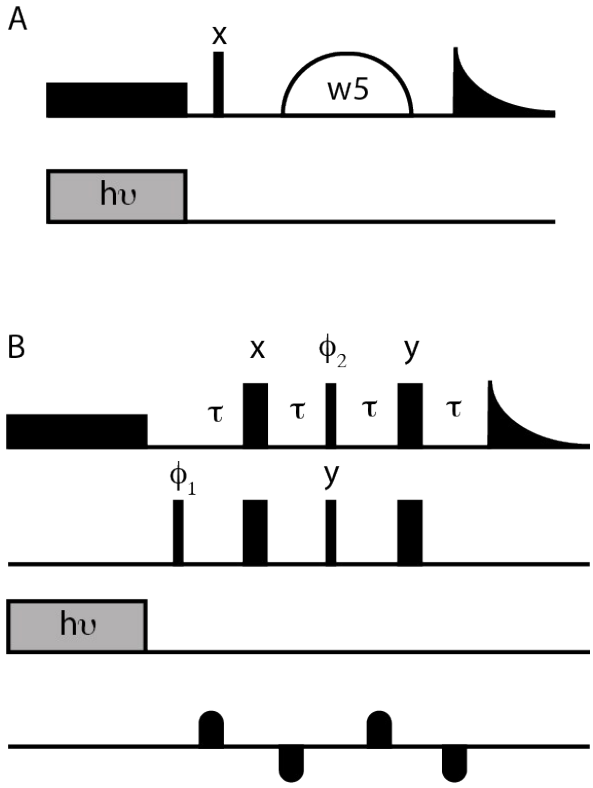

Figure S14: Photo-CIDNP experiments. A simultaneous pre-saturation pulse with a light irradiation of 4 seconds is applied in both pulse programs A) 1D ^{1}H enhanced photo-CIDNP experiment, with w5 representing a Watergate w5 block. B) ^{13}C enhanced ^{1}H detected photo-CIDNP experiment, with τ=1.7 ms; φ1=x, -x; and φ2=x, -x. The gradient power was set to 33%. The receiver phase was set to x, -x, -x, x, -y, y, y, -y.

References

1. Liu, M. L.; Mao, X. A.; Ye, C. H.; Huang, H.; Nicholson, J. K.; Lindon, J. C., Improved WATERGATE pulse sequences for solvent suppression in NMR spectroscopy. *J Magn Reson* **1998,** *132* (1), 125-129.
2. Improta, R.; Barone, V., Interplay of electronic, environmental, and vibrational effects in determining the hyperfine coupling constants of organic free radicals. *Chemical Reviews* **2004,** *104* (3), 1231-1253.
3. Kiryutin, A. S.; Morozova, O. B.; Kuhn, L. T.; Yurkovskaya, A. V.; Hore, P. J., H-1 and C-13 hyperfine coupling constants of the Tryptophanyl cation radical in aqueous solution from microsecond time-resolved CIDNP. *Journal of Physical Chemistry B* **2007,** *111* (38), 11221-11227.
4. Morozova, O. B.; Ivanov, K. L.; Kiryutin, A. S.; Sagdeev, R. Z.; Kochling, T.; Vieth, H. M.; Yurkovskaya, A. V., Time-resolved CIDNP: an NMR way to determine the EPR parameters of elusive radicals. *Phys Chem Chem Phys* **2011,** *13* (14), 6619-27.
5. Morozova, O. B.; Panov, M. S.; Fishman, N. N.; Yurkovskaya, A. V., Electron transfer vs. proton-coupled electron transfer as the mechanism of reaction between amino acids and triplet-excited benzophenones revealed by time-resolved CIDNP. *Phys Chem Chem Phys* **2018,** *20* (32), 21127-21135.
6. Saprygina, N. N.; Morozova, O. B.; Grampp, G.; Yurkovskaya, A. V., Effect of Amino Group Charge on the Photooxidation Kinetics of Aromatic Amino Acids. *J. Phys. Chem. A* **2014,** *118* (2), 339-349.
7. Morozova, O. B.; Panov, M. S.; Fishman, N. N.; Yurkovskaya, A. V., Electron transfer vs proton-coupled electron transfer as the mechanism of reaction between amino acids and triplet-excited benzophenones revealed by time-resolved CIDNP. *Phys. Chem. Chem. Phys.* **2018,** *20* (32), 21127-21135.
8. Wilson, D. J. D.; Mohn, C. E.; Helgaker, T., The rotational g tensor as a benchmark for density-functional theory calculations of molecular magnetic properties. *J Chem Theory Comput* **2005,** *1* (5), 877-888.
9. Sobol, A.; Torres, F.; Aicher, A.; Renn, A.; Riek, R., Atto Thio 12 as a promising dye for photo-CIDNP. *J Chem Phys* **2019,** *151* (23), 234201.
10. Lee, J. H.; Sekhar, A.; Cavagnero, S., H-1-Detected C-13 Photo-CIDNP as a Sensitivity Enhancement Tool in Solution NMR. *Journal of the American Chemical Society* **2011,** *133* (21), 8062-8065.